Conjugated Polycycles

DOI: 10.1002/anie.201403509

Heptagon-Embedded Pentacene: Synthesis, Structures, and Thin-Film Transistors of Dibenzo[*d*,*d*′]benzo[1,2-*a*:4,5-*a*′]dicycloheptenes**

*Xuejin Yang, Danqing Liu, and Qian Miao**

Abstract: *This study presents a new class of conjugated polycyclic molecules that contain seven-membered rings, detailing their synthesis, crystal structures and semiconductor properties. These molecules have a nearly flat* C_6-C_7-C_6-C_7-C_6 *polycyclic framework with a p-quinodimethane core. With field-effect mobilities of up to* $0.76\,cm^2\,V^{-1}\,s^{-1}$ *as measured from solution-processed thin-film transistors, these molecules are alternatives to the well-studied pentacene analogues for applications in organic electronic devices.*

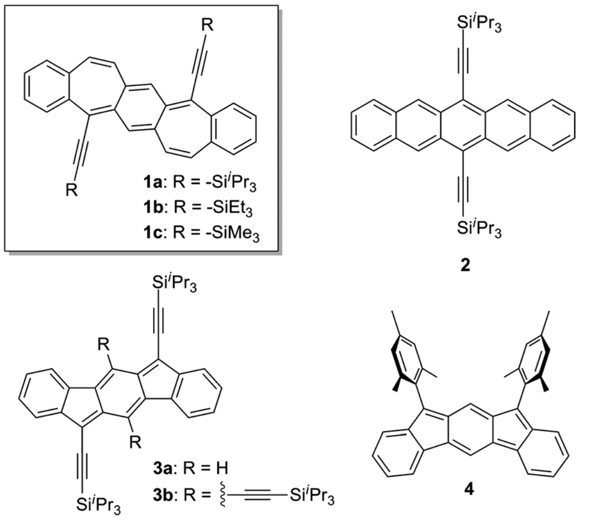

Figure 1. Structures of ethynylated dibenzo[*d*,*d*′]benzo[1,2-*a*:4,5-*a*′]-dicycloheptenes (**1a–c**) and related molecules.

Conjugated polycyclic hydrocarbons containing non-hexagonal carbocycles[1] have received considerable attention in organic chemistry and materials science because of their novel properties and potential applications. The most widely studied subgroup of these conjugated polycyclic hydrocarbons contains five-membered rings. This group of molecules include curved π-conjugated molecules known as aromatic bowls[2,3] (or buckybowls[4]) and electron acceptors[5] as applied in organic electronics, since the five-membered rings can not only introduce positive curvature but also stabilize injected electrons by forming the aromatic cyclopentadienyl anion. Unlike five-membered rings, seven-membered rings can give rise to saddle-shaped π-molecules with negative curvature[6] and stabilize holes injected into p-type organic semiconductors by forming the aromatic cycloheptatrienyl cation.[7] However, conjugated polycyclic hydrocarbons containing seven-membered rings have been rarely explored. Herein, we report dibenzo[*d*,*d*′]benzo[1,2-*a*:4,5-*a*′]dicycloheptene derivatives (**1a–c**, Figure 1),[8] which have an unprecedented pentacyclic conjugated backbone containing two seven-membered carbocycles.[9] Unlike the recently reported indenofluorenes (**3a**,**b** and **4**, Figure 1),[10] **1a–c** have seven-membered rings rather than five-membered rings replacing two benzene rings in pentacene, a benchmark organic semiconductor for applications in organic thin-film transistors (OTFTs). The synthesis, X-ray crystal structures and OTFTs containing compounds **1a–c** are described.

Scheme 1 details the synthesis of molecules **1a–c** starting from compound **5**,[11] which was prepared from *p*-xylene in four steps by modification of reported methods.[12] Cyanation of compound **5** was achieved by heating with CuCN to reflux in DMF to form **6** as a mixture of isomers, which were used in the subsequent catalytic hydrogenation without separation. In contrast, lithiation of molecule **5** followed by reaction with CO_2 afforded the corresponding diacid in very poor yield, and subsequent catalytic hydrogenation of **5** led to debromination. Hydrolysis of dicyanide **7** resulted in the diacid **8**. The total yield of **8** from *p*-xylene in seven steps was 49%. In comparison to this synthesis, the earlier reported preparation of **8** from phenylacetic acid and pyromellitic dianhydride required fewer steps but had a much lower total yield (14%), and involved a byproduct that could lead to explosion.[13] Double cyclization of diacid **8** with polyphosphonic acid at elevated temperature and subsequent dehydrogenation yielded dione **10**, which was first reported 40 years ago[13] but almost neglected afterwards. Addition of various acetylide compounds to **10** produced diols **11a–c**. Subsequent reduction of the intermediate diol **11a** in THF with a solution of 37% HCl that was saturated with $SnCl_2$ led to the formation of a deep purple solution, from which **1a** was isolated as a stable compound in good yield. The same

---

[*] X. Yang, D. Liu, Prof. Q. Miao
Department of Chemistry,
The Chinese University of Hong Kong
Shatin, New Territories, Hong Kong (China)
E-mail: miaoqian@cuhk.edu.hk
Prof. Q. Miao
Institute of Molecular Functional Materials
(Areas of Excellence Scheme, University Grants Committee)
Hong Kong (China)

[**] We thank Hoi Shan Chan (the Chinese University of Hong Kong) for the single-crystal X-ray crystallography. This work was supported by the Research Grants Council of Hong Kong (project number: GRF402412) and the University Grants Committee of Hong Kong (project number: AoE/P-03/08).

Supporting information for this article is available on the WWW under http://dx.doi.org/10.1002/anie.201403509.

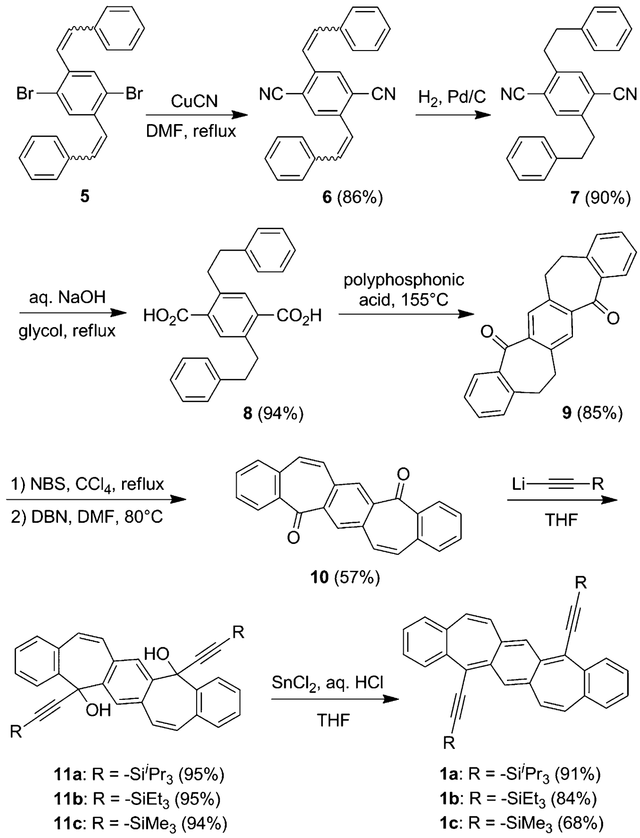

Scheme 1. Synthesis of **1a**–**c**. NBS = *N*-bromosuccinimide. DBN = 1,5-diazabicyclo[4.3.0]non-5-ene.

method was used to prepare **1b** and **1c** from diols **11b** and **11c**, respectively, with lower yields.

Two findings related to the stability of **1a**–**c** should be noted. First, **1a**–**c** appeared unstable on common silica gel or neutral alumina for unknown reasons. However, these compounds were successfully purified with column chromatography using silica gel or neutral alumina that were deactivated with 6% of water (detailed in the Supporting Information). Second, it was necessary to keep the concentration of **11b**,**c** at 2 mM or lower to achieve a good yield of **1b**,**c**. When the concentration of **11b**,**c** in THF was higher, the yield of **1b**,**c** decreased dramatically and the ^{1}H NMR spectra of the crude products exhibited broad signals, which suggested polymerization of **1b**,**c** under the acidic conditions. To further investigate this observation, the stability of **1a**–**c** in solution (concentration 0.02 M) was monitored with ^{1}H NMR spectroscopy. It was found that after storage of the solutions under ambient conditions for six days, no changes were apparent in the ^{1}H NMR spectra of the solutions of **1a** and **1b** in CDCl$_3$ (Supporting Information). In contrast, the solution of **1c** in CDCl$_3$ turned dark red and exhibited a broad signal in the aromatic region of the ^{1}H NMR spectra after storage under the same conditions for one day. The instability of **1c** may be related to polymerization of the reactive C–C double bonds in the π-conjugated backbone. In contrast, compounds **1a** and **1b** are more stable, likely because their larger substituents can hinder polymerization by blocking overlap of the reactive C–C double bonds.

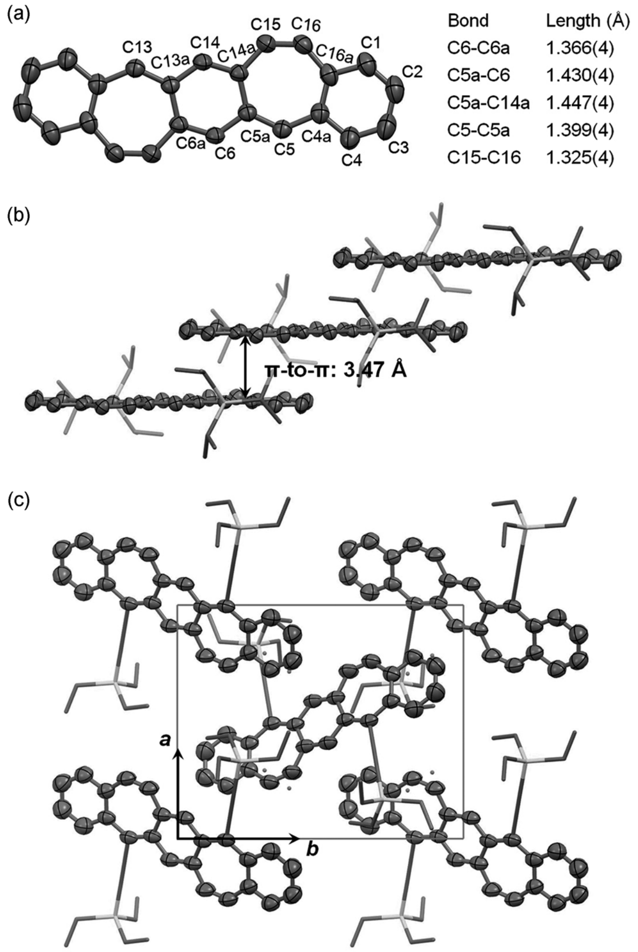

Figure 2. a) The pentacyclic backbone of **1a** in the crystal structure with partial carbon-atom labeling and some highlighted bond lengths; b) π-stacking between **1a** molecules in the single crystal; c) molecular packing of **1b** as viewed along the *c*-axis of the unit cell. (Hydrogen atoms are removed for clarity. Thermal ellipsoids set at 50% probability, silylethynyl substituents are shown as capped sticks, and disordered triethyl groups of **1b** are shown as dots.)

Crystals of **1a** and **1b** suitable for single-crystal X-ray analysis were grown from solutions in hexane and ethyl acetate.[14] Figure 2a shows the pentacyclic backbone of **1a**, which is essentially flat. Examination of the bond lengths indicates that the central six-membered ring has two short C–C bonds (C6–C6a and C14–C14a: 1.37 Å) and four long C–C bonds (C5a–C6 and C13a–C14: 1.43 Å; C5a–C14a and C6a–C13a: 1.45 Å) and is bonded to C5 and C13 by relatively short bonds (C5–C5a and C13–C13a: 1.40 Å). These bond lengths are similar to the corresponding bond lengths in the crystal structure of **3b**,[10a] and are in agreement with a *p*-quinodimethane structure. The seven-membered ring contains a C–C double bond (C15–C16) which measures 1.33 Å, a typical bond length for alkenes. In comparison, the C5–C4a, C14a–C15, and C16–C16a bonds in the seven-membered ring measure 1.44–1.48 Å and resemble single bonds between two sp^2-hybridized carbon atoms.[15] Unlike its pentacene analogue **2** (Figure 1),[16] which stacks in a two-dimensional face-to-face π-stacking arrangement, compound **1a** forms one-dimensional offset π-stacks (Figure 2b). In each stack, two parallel neighbors have roughly two rings overlapped with a π-to-π distance of 3.47 Å. The non-overlapped space above and below the pentacyclic backbone is occupied by the triisopropylsilyl groups of neighboring stacks. The fact that **1a** forms one-dimensional π-stacks rather than two-dimensional π-stacks is likely related to the substitution position of bulky triisopropylsilyl groups. With a smaller substituting group, **1b** exhibits a special herringbone-type arrangement (shown in Figure 2c), where one molecule of **1b** has the edge of its termini contacted with the π-face of a neighboring molecule. This packing motif involves much less intermolecular overlap of π-orbitals than the established herringbone packing of pentacene.

Molecules **1a–c** are deep purple and nonfluorescent in solution when excited with UV light, and exhibit almost identical UV/Vis absorption spectra. The UV/Vis absorption spectra of compounds **1a** and **2** are shown in Figure 3 for comparison. In the visible-light region, **1a** exhibits more intense absorption than **2**. The longest wavelength absorption maxima of **1a** occurs at $\lambda = 587$ nm, which is blue-shifted by 55 nm relative to that of **2**. To determine the energy levels of the highest occupied molecular orbital (HOMO) and the lowest unoccupied molecular orbital (LUMO), the redox behavior of compound **1a** in solution in dichloromethane was investigated with cyclic voltammetry. The cyclic voltammogram of **1a** (Supporting Information) exhibited a reversible reduction wave and a reversible oxidation wave with half-wave potentials of −1.66 V and 0.12 V versus ferrocene/ferrocenium, respectively. Based on these electrochemical potentials, the HOMO and LUMO energy levels of **1a** are estimated as −4.92 eV and −3.14 eV, respectively.[17] These energy levels lead to a HOMO–LUMO energy gap of 1.78 eV, which is in good agreement with the absorption edge at approximately $\lambda = 649$ nm (1.91 eV). In comparison, the HOMO and LUMO energy levels of **2**, also estimated from electrochemical potentials, are −5.17 eV and −3.30 eV, respectively,[18] and the HOMO and LUMO energy levels of **3a** are −5.88 eV and −4.00 eV, respectively.[10b] The higher HOMO and LUMO energy levels of **1a** correspond to the fact that the seven-membered ring in **1a** is more easily oxidized than the benzene ring in **2** and the five-membered ring in **3a** by forming an aromatic cycloheptatrienyl cation.

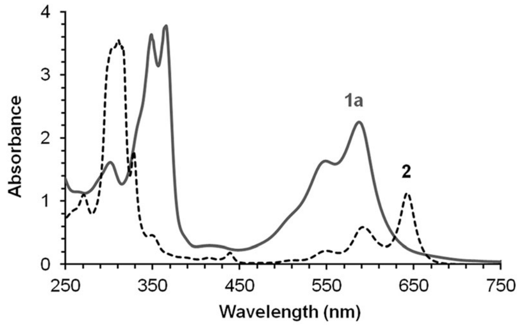

Figure 3. UV/Vis absorption spectra of 0.05 mM solutions of **1a** and **2** in dichloromethane.

To test the semiconductor properties of **1a–c**, thin-film transistors of **1a–c** were fabricated by dip-coating or drop-casting a solution onto an oxidized silicon substrate. High-quality films of **1a** were formed by immersing a SiO_2/Si substrate in a solution of **1a** (2 mg mL^{-1}) in a solvent mixture of dichloromethane and acetone (1:1 by volume) and then pulling it up with a constant speed of 5.4 μm s^{-1}. The films of **1a** deposited on the SiO_2 surface were composed of aligned crystalline fibers, as shown in the polarized-light micrograph of Figure 4a. X-ray diffraction patterns from the films of **1a** (Supporting Information) exhibited one peak at a *d*-spacing of 11.19 Å ($2\theta = 7.90°$) and three higher-order peaks at *d*-spacings of 5.59 Å, 3.72 Å, and 2.79 Å. These peaks do not correspond to any diffractions derived from the single-crystal structure of **1a**, and thus indicate a polymorph different from its bulk crystals. The device fabrication was completed by depositing a layer of gold on the film of **1a** through a shadow mask to form top-contact source and drain electrodes. As measured in air from these devices, **1a** functioned as a p-type semiconductor with a field-effect mobility in the range of 0.19–0.76 cm^2 V^{-1} s^{-1}. The highest mobility was extracted from the transfer *I–V* curves shown in Figure 4b using the equation: $I_{DS} = (\mu W C_i / 2L)(V_G - V_T)^2$, where I_{DS} is the drain current, μ is field-effect mobility, C_i is the capacitance per unit area (11 nF cm^{-2}) for the 300 nm-thick dielectric layer of SiO_2, W is the channel width, L is the channel length, and V_G and V_T are the gate and threshold voltage, respectively. It was found that the mobility of 0.76 cm^2 V^{-1} s^{-1} decreased to 0.57 cm^2 V^{-1} s^{-1} and 0.39 cm^2 V^{-1} s^{-1} after the device was stored in air for one week and one month, respectively. Such degradation of mobility can be attributed to the fact that the thin-film phase gradually changes to the more stable bulk-crystal phase. This is shown by the X-ray diffractions from the film stored for one week (Supporting Information), which indicate the existence of both the thin-film phase and the bulk-crystal phase of **1a**. The thin-film transistors of **1b** and **1c** exhibited field-effect mobilities of 6×10^{-4} and 5×10^{-5} cm^2 V^{-1} s^{-1}, respectively, for holes. The low mobility of

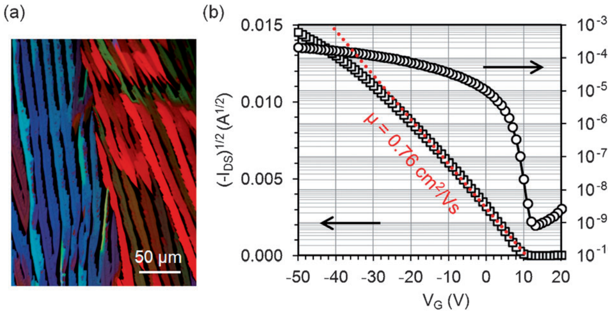

Figure 4. a) Reflection polarized-light micrograph of a film of **1a** as dip-coated on SiO_2 at a substrate temperature of room temperature. b) Drain current (I_{DS}) versus gate voltage (V_G) with drain voltage (V_{DS}) at −50 V for the best-performing OTFT of **1a** measured in air with an active channel of $W = 1$ mm and $L = 50$ μm.

1b is in agreement with its molecular packing, which only has poor edge-to-face interactions between the π-backbone of neighboring molecules.

The device exhibits a positive threshold voltage of approximately 10 V and a large drain current of circa 1×10^{-5} A at zero gate bias (Figure 4b). The drain current is suppressed by a positive gate voltage of 12 V to approximately 1×10^{-9} A, which corresponds to an on/off ratio of greater than 10^5 when compared with the on-current obtained at a gate voltage of −50 V. The large drain current at zero gate bias and the positive threshold voltage of **1a** are similar to those of the solution-processed OTFTs of **2** reported earlier,[19] and indicate that the film of **1a** is already p-doped at zero gate bias. This observation is in agreement with the fact that molecule **1a** has an even higher HOMO energy level than **2**. To identify the possible dopants, the thin-film transistors of **1a** were then tested under vacuum. It was found that under vacuum the transistor of **1a** exhibited essentially the same drain current of approximately 1×10^{-5} A at zero gate bias, suggesting that the film is doped not by oxygen from the air but likely by oxygen species on the SiO_2 dielectric surface. To test this hypothesis, the SiO_2 surface was pretreated with a self-assembled monolayer (SAM) of organosilane. As shown in the Supporting Information, when the SiO_2 surface was modified with phenyltrichlorosilane,[20] the drain current at zero gate bias was reduced to circa 1×10^{-8} A and the threshold voltage shifted to approximately 3 V. This change is probably because the oxygen species on the SiO_2 were passivated by the SAM of phenyltrichlorosilane. When the SiO_2 was modified with 3-(aminopropyl)triethoxysilane,[21] the drain current at zero gate bias was further reduced to approximately 1×10^{-10} A and the threshold voltage shifted to −26 V. This change occurs because the surface amino groups are known to cause a shift in threshold voltage to more negative values, presumably by electron transfer into organic semiconductors.

In summary, this study puts forth a new class of conjugated polycyclic molecules that contain a linearly annulated C_6-C_7-C_6-C_7-C_6 polycyclic framework. The crystal structures of **1a** and **1b** indicate that their pentacyclic π-backbone is nearly flat with a *p*-quinodimethane core. With bulky substituents, **1a** and **1b** exhibit robust environmental stability in solution. It is found that **1a**–**c** function as p-type organic semiconductors in solution-processed OTFTs with field-effect mobilities of up to 0.76 $cm^2\,V^{-1}\,s^{-}$. These results suggest that heptagon-embedded conjugated polycyclic hydrocarbons are promising candidates for organic electronic materials.

Received: March 20, 2014

Keywords: conjugation · organic electronics · polycyclic aromatic hydrocarbons · semiconductors · seven-membered ring

---

[1] For recent examples of conjugated polycyclic hydrocarbons containing four- and eight-membered rings, see: a) Bharat, R. Bhola, T. Bally, A. Valente, M. K. Cyrański, Ł. Dobrzycki, S. M. Spain, P. Rempała, M. R. Chin, B. T. King, *Angew. Chem.* **2010**, *122*, 409–412; *Angew. Chem. Int. Ed.* **2010**, *49*, 399–402; b) C.-N. Feng, M.-Y. Kuo, Y.-T. Wu, *Angew. Chem.* **2013**, *125*, 7945–7948; *Angew. Chem. Int. Ed.* **2013**, *52*, 7791–7794.

[2] a) Y. T. Wu, J. S. Siegel, *Chem. Rev.* **2006**, *106*, 4843–4867; b) L. T. Scott, *Polycyclic Aromat. Compd.* **2010**, *30*, 247–259.

[3] For recent examples, see: a) B. D. Steinberg, E. A. Jackson, A. S. Filatov, A. Wakamiya, M. A. Petrukhina, L. T. Scott, *J. Am. Chem. Soc.* **2009**, *131*, 10537–10545; b) T. Amaya, T. Nakata, T. Hirao, *J. Am. Chem. Soc.* **2009**, *131*, 10810–10811; c) A. C. Whalley, K. N. Plunkett, A. A. Gorodetsky, C. L. Schenck, C.-Y. Chiu, M. L. Steigerwald, C. Nuckolls, *Chem. Sci.* **2011**, *2*, 132; d) T. Amaya, T. Hirao, *Chem. Commun.* **2011**, *47*, 10524–10535; e) T.-C. Wu, M.-K. Chen, Y.-W. Lee, M.-Yu. Kuo, Y.-T. Wu, *Angew. Chem.* **2013**, *125*, 1327–1331; *Angew. Chem. Int. Ed.* **2013**, *52*, 1289–1293.

[4] P. W. Rabideau, A. Sygula, *Acc. Chem. Res.* **1996**, *29*, 235–242.

[5] a) F. G. Brunetti, X. Gong, M. Tong, A. J. Heeger, F. Wudl, *Angew. Chem.* **2010**, *122*, 542–546; *Angew. Chem. Int. Ed.* **2010**, *49*, 532–536; b) D. T. Chase, A. G. Fix, S. J. Kang, B. D. Rose, C. D. Weber, Y. Zhong, L. N. Zakharov, M. C. Lonergan, C. Nuckolls, H. M. Haley, *J. Am. Chem. Soc.* **2012**, *134*, 10349–10352; c) J. Nishida, S. Tsukaguchi, Y. Yamashita, *Chem. Eur. J.* **2012**, *18*, 8964–8970; d) J. D. Wood, J. L. Jellison, A. D. Finke, L. Wang, K. N. Plunkett, *J. Am. Chem. Soc.* **2012**, *134*, 15783–15789; e) J. L. Jellison, C.-H. Lee, X. Zhu, J. D. Wood, K. N. Plunkett, *Angew. Chem.* **2012**, *124*, 12487–12490; *Angew. Chem. Int. Ed.* **2012**, *51*, 12321–12324; f) H. Xia, D. Liu, X. Xu, Q. Miao, *Chem. Commun.* **2013**, *49*, 4301–4303.

[6] a) K. Yamamoto, T. Harada, M. Nakazaki, *J. Am. Chem. Soc.* **1983**, *105*, 7171–7172; b) K. Yamamoto, T. Harada, Y. Okamoto, H. Chikamatsu, M. Nakazaki, Y. Kai, T. Nakao, M. Tanaka, S. Harada, N. Kasai, *J. Am. Chem. Soc.* **1988**, *110*, 3578–3584; c) K. Yamamoto, Y. Saitho, D. Iwaki, T. Ooka, *Angew. Chem.* **1991**, *103*, 1202–1203; *Angew. Chem. Int. Ed. Engl.* **1991**, *30*, 1173–1174; d) J. Luo, X. Xu, R. Mao, Q. Miao, *J. Am. Chem. Soc.* **2012**, *134*, 13796–13803; e) K. Kawasumi, Q. Zhang, Y. Segawa, L. T. Scott, K. Itami, *Nat. Chem.* **2013**, *5*, 739–744.

[7] H. Xia, D. Liu, K. Song, Q. Miao, *Chem. Sci.* **2011**, *2*, 2402–2406.

[8] Dibenzo[*d*,*d'*]benzo[1,2-*a*:4,5-*a'*]dicycloheptene is the name recommended by the ACS. According to recent IUPAC nomenclature (1998), it should be named as dibenzo[*d*,*d'*]benzo[1,2-*a*:4,5-*a'*]di[7]annulene.

[9] A similar pentacyclic conjugated backbone of boron-substituted heteroarenes has two fewer π-electrons than molecules **1a**–**c**. See: A. J. Caruso, M. A. Siegler, J. D. Tovar, *Angew. Chem.* **2010**, *122*, 4309–4313; *Angew. Chem. Int. Ed.* **2010**, *49*, 4213–4217.

[10] a) D. T. Chase, B. D. Rose, S. P. McClintock, L. N. Zakharov, M. M. Haley, *Angew. Chem.* **2011**, *123*, 1159–1162; *Angew. Chem. Int. Ed.* **2011**, *50*, 1127–1130; b) D. T. Chase, A. G. Fix, B. D. Rose, C. D. Weber, S. Nobusue, C. E. Stockwell, L. N. Zakharov, M. C. Lonergan, M. M. Haley, *Angew. Chem.* **2011**, *123*, 11299–11302; *Angew. Chem. Int. Ed.* **2011**, *50*, 11103–11106; c) A. Shimizu, Y. Tobe, *Angew. Chem.* **2011**, *123*, 7038–7042; *Angew. Chem. Int. Ed.* **2011**, *50*, 6906–6910.

[11] R. Umeda, S. Miyake, Y. Nishiyama, *Chem. Lett.* **2012**, *41*, 215–217.

[12] a) M. C. Bonifacio, C. R. Robertson, J.-J. Jung, B. T. King, *J. Org. Chem.* **2005**, *70*, 8522–8526; b) Z. Shi, X. Zhang, G. Yang, Z. Su, Z. Cui, *Tetrahedron* **2011**, *67*, 4110–4117.

[13] I. Agranat, D. Avnir, *J. Chem. Soc. Perkin Trans. 1* **1974**, 1155–1161.

[14] CCDC 992241 (**1a**) and 992242 (**1b**) contain the supplementary crystallographic data for this paper. These data can be obtained free of charge from The Cambridge Crystallographic Data Centre via www.ccdc.cam.ac.uk/data_request/cif.

[15] The typical bond length for a single bond between two sp^2-hybridized carbon atoms is 1.45–1.46 Å. See: E. V. Anslyn, D. A. Dougherty, *Modern Physical Organic Chemistry*, University Science Books, Sausalito, **2004**, chap. 1, p. 22.

[16] a) J. E. Anthony, J. S. Brooks, D. L. Eaton, S. R. Parkin, *J. Am. Chem. Soc.* **2001**, *123*, 9482–9483.

[17] The commonly used HOMO energy level of ferrocene is −4.80 eV, which is calculated on the basis of an approximation, neglecting solvent effects, using a work function of 4.6 eV for the standard hydrogen electrode (SHE) and an electrochemical potential of 0.2 V for the ferrocene/ferrocenium couple versus SHE. See: a) J. Pommerehne, H. Vestweber, W. Guss, R. F. Mahrt, H. Bässler, M. Porsch, J. Daub, *Adv. Mater.* **1995**, *7*, 551–554; b) B. W. D'Andrade, S. Datta, S. R. Forrest, P. Djurovich, E. Polikarpov, M. E. Thompson, *Org. Electron.* **2005**, *6*, 11–20.

[18] Z. Liang, Q. Tang, J. Xu, Q. Miao, *Adv. Mater.* **2011**, *23*, 1535–1539.

[19] a) M. M. Payne, S. R. Parkin, J. E. Anthony, C.-C. Kuo, T. N. J. Jackson, *J. Am. Chem. Soc.* **2005**, *127*, 4986–4987; b) S. K. Park, T. N. Jackson, J. E. Anthony, D. A. Mourey, *Appl. Phys. Lett.* **2007**, *91*, 063514.

[20] G. Giri, E. Verploegen, S. C. B. Mannsfeld, S. Atahan-Evrenk, D. H. Kim, S. Y. Lee, H. A. Becerril, A. Aspuru-Guzik, M. F. Toney, Z. Bao, *Nature* **2011**, *480*, 504–508.

[21] S. Kobayashi, T. Nishikawa, T. Takenobu, S. Mori, T. Shimoda, T. Mitani, H. Shimotani, N. Yoshimoto, S. Ogawa, Y. Iwasa, *Nat. Mater.* **2004**, *3*, 317–322.